Electronic Supplementary Information

Syntheses, Crystal structures, DNA Binding, DNA cleavage, Molecular docking and DFT study of Cu(II) Complexes involving N_2O_2 Donor azo Schiff Base Ligands

Saikat Banerjee,[a] Pravat Ghorai,[a] Paula Brandão,[b] Dipanjan Ghosh,[c] Sutanwi Bhuiya,[a] Dhrubajyoti Chattopadhyay,[d] Suman Das,[a] and Amrita Saha[*a]

[a]*Department of Chemistry, Jadavpur University, Kolkata- 700032, India.*

E-mail: asaha@chemistry.jdvu.ac.in;amritasahachemju@gmail.com; Tel. +91-33-24572941

[b]*Departamento de Química, CICECO, Universidade de Aveiro, 3810-193 Aveiro, Portugal.*

[c]*NIPER, Kolkata – 700032, India.*

[d]*Amity University, Kolkata – 700135, India.*

CONTENTS:

Table S1. Mulliken atomic charge distribution of complexes **1-3.**

1	**2**	**3**
1 Cu 0.641000	1 Cu 0.644754	1 Cu 0.634335
2 O -0.595882	2 O -0.597327	2 O -0.570445
3 C 0.362464	3 C 0.358604	3 C 0.360001
4 C 0.307903	4 C 0.302458	4 C 0.305248
5 C -0.056564	5 C -0.061827	5 C -0.064484
7 C 0.210291	7 C 0.216886	7 C 0.219126
8 C -0.076005	8 C -0.078959	8 C -0.085174
10 C 0.050828	10 C 0.054495	10 C 0.054611
11 O -0.489993	11 O -0.476857	11 O -0.481588
12 C 0.293281	12 C 0.300513	12 C 0.298041
16 N -0.274272	16 N -0.274112	16 N -0.259053
17 N -0.290011	17 N -0.287548	17 N -0.278491
18 C 0.224129	18 C 0.223869	18 C 0.227325
19 C 0.001864	19 C -0.002869	19 C -0.010461
21 C -0.066204	21 C -0.009278	21 C -0.002850
23 C 0.135162	23 C 0.026014	23 C 0.009431
24 C -0.074754	25 C -0.019417	25 C -0.004533
26 C 0.022393	27 C 0.020835	27 C 0.004943
28 C 0.006665	29 C 0.226611	29 C 0.244966
32 C 0.242852	31 N -0.488017	31 N -0.513696
34 N -0.484028	32 C 0.223720	32 C 0.228901
35 C 0.221068	35 C 0.002094	35 C 0.026308
38 O -0.207303	36 C 0.022677	38 C 0.228998
40 C 0.250423	40 C 0.020471	41 N -0.494417
43 N -0.493551	44 C 0.222859	42 C 0.238586
44 C 0.231618	47 N -0.492348	44 C 0.052915
46 C 0.053164	48 C 0.224709	45 C 0.361935
47 C 0.361167	50 C 0.054980	46 C 0.295427
48 C 0.305869	51 C 0.364116	47 C -0.061213
49 C -0.062651	52 C 0.303668	49 C 0.220355
51 C 0.219732	53 C -0.063522	50 C -0.076192
52 C -0.084707	55 C 0.227057	52 O -0.587532
54 O -0.590489	56 C -0.082607	53 O -0.452550
55 O -0.483645	58 O -0.585175	54 C 0.283523
56 C 0.292802	59 O -0.483952	58 N -0.275721
60 N -0.270175	60 C 0.296443	59 N -0.287497
61 N -0.286409	64 N -0.276192	60 C 0.225209
62 C 0.221938	65 N -0.289992	61 C 0.019852
63 C -0.002543	66 C 0.221658	63 C -0.016334

65 C -0.058767 67 C 0.130653 68 C -0.071241 70 C 0.019143 72 C 0.007530 76 C 0.205253 Sum of Mulliken charges with hydrogens summed into heavy atoms = 0.00000	67 C 0.019839 69 C -0.010268 71 C 0.010389 73 C -0.003358 75 C -0.006096 Sum of Mulliken charges with hydrogens summed into heavy atoms = 0.00000	65 C 0.024119 67 C -0.005633 69 C -0.008385 71 O -0.027906 Sum of Mulliken charges with hydrogens summed into heavy atoms = 0.00000

Table S2. Energy (eV) and composition (%) of selected M.O.s of complex **1**

M.O.s (α-spin)	Energy(eV)	% Metal	% Ligand	**M.O.s (β-spin)**	Energy(eV)	% Metal	% Ligand
LUMO+5	-0.57	22	78	LUMO+5	-1.91	17	83
LUMO+4	-1.99	14	86	LUMO+4	-2.29	8	92
LUMO+3	-2.35	6	94	LUMO+3	-2.45	6	94
LUMO+2	-2.57	2	98	LUMO+2	-2.77	3	97
LUMO+1	-2.77	2	98	LUMO+1	-3.82	49	51
LUMO	-4.11	55	45	LUMO	-4.06	49	51
HOMO	-5.54	40	60	HOMO	-5.92	53	47
HOMO-1	-6.12	55	45	HOMO-1	-6.35	73	27
HOMO-2	-6.48	71	29	HOMO-2	-6.56	0	100
HOMO-3	-6.56	0	100	HOMO-3	-6.6	11	89
HOMO-4	-6.67	9	91	HOMO-4	-6.68	0	100
HOMO-5	-6.68	1	99	HOMO-5	-6.71	8	92

Table S3.Energy (eV) and composition (%) of selected M.O.s of complex **2**

M.O.s (α-spin)	Energy(eV)	% Metal	% Ligand	**M.O.s (β-spin)**	Energy(eV)	% Metal	% Ligand
LUMO+5	0.15	25	75	LUMO+5	0.14	15	85
LUMO+4	0.14	12	88	LUMO+4	-1.53	10	90
LUMO+3	-1.57	7	93	LUMO+3	-1.54	5	95
LUMO+2	-1.58	0	100	LUMO+2	-1.76	4	96
LUMO+1	-1.76	3	97	LUMO+1	-1.78	51	49
LUMO	-1.79	58	42	LUMO	-2.95	47	53
HOMO	-5.08	43	5	HOMO	-5.04	57	43
HOMO-1	-5.19	51	49	HOMO-1	-5.19	77	23
HOMO-2	-5.84	77	23	HOMO-2	-5.84	3	97
HOMO-3	-5.84	7	93	HOMO-3	-5.84	17	83
HOMO-4	-6.27	9	91	HOMO-4	-6.27	10	90
HOMO-5	-6.27	5	95	HOMO-5	-6.27	0	100

Table S4. Energy (eV) and composition (%) of selected M.O.s of complex **3**

M.O.s (α-spin)	Energy(eV)	% Metal	% Ligand	**M.O.s (β-spin)**	Energy(eV)	% Metal	% Ligand
LUMO+5	0.16	23	77	LUMO+5	0.15	16	84
LUMO+4	0.15	12	88	LUMO+4	-1.48	5	95
LUMO+3	-1.52	7	93	LUMO+3	-1.52	4	96
LUMO+2	-1.55	4	96	LUMO+2	-1.68	4	96
LUMO+1	-1.69	3	97	LUMO+1	-1.72	45	55
LUMO	-1.72	60	40	LUMO	-2.94	42	58
HOMO	-5.02	37	63	HOMO	-4.98	59	41
HOMO-1	-5.12	55	45	HOMO-1	-5.12	75	25
HOMO-2	-5.78	77	23	HOMO-2	-5.78	0	100
HOMO-3	-5.8	0	100	HOMO-3	-5.8	10	90
HOMO-4	-6.17	0	100	HOMO-4	-6.16	7	93
HOMO-5	-6.19	1	99	HOMO-5	-6.18	11	89

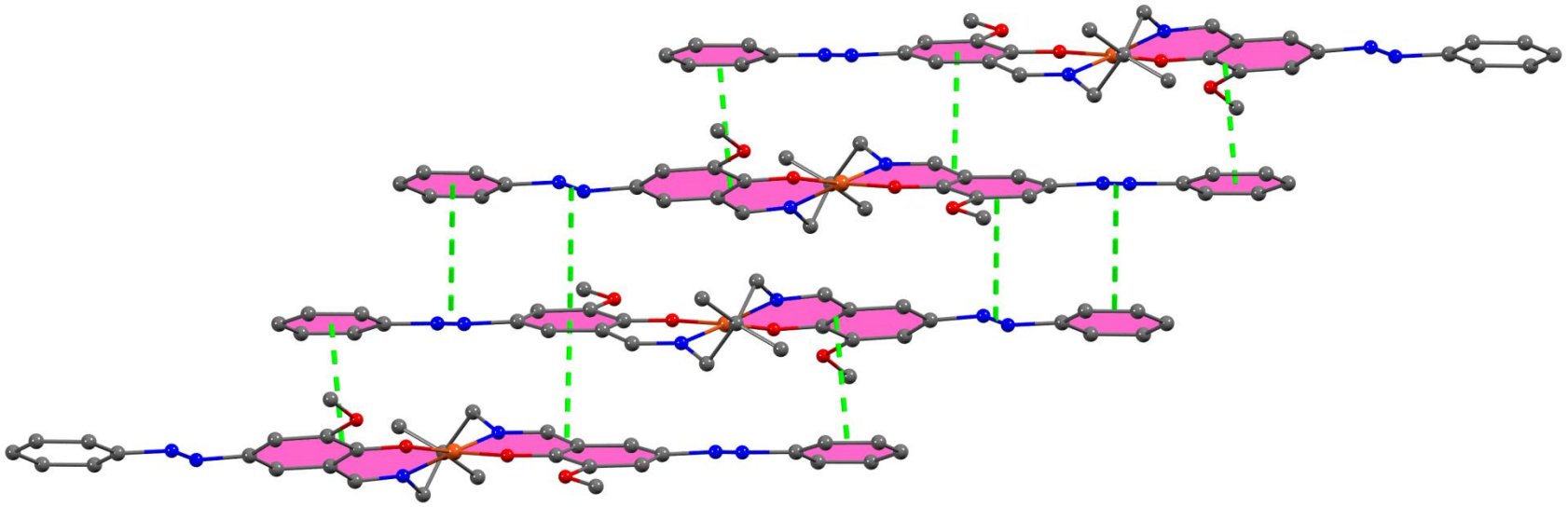

Fig.S1. 1D supramolecular architecture of complex **2**propagating along the *b axis* showing π–π stacking interaction.Hydrogen atoms of least interest are omitted for clarity.

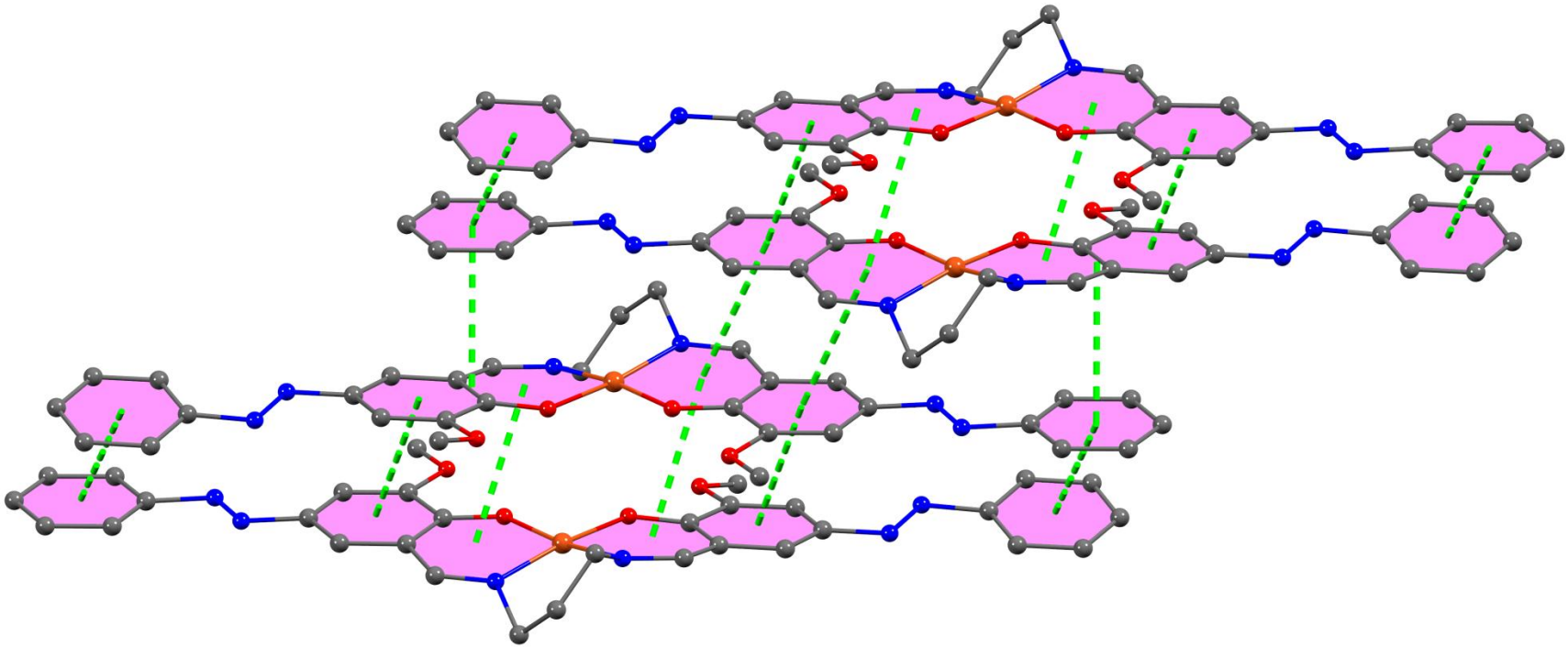

Fig.S2. 1D supramolecular architecture of complex **3**propagating along the *b axis* showing π–π stacking interaction. Hydrogen atoms of least interest are omitted for clarity

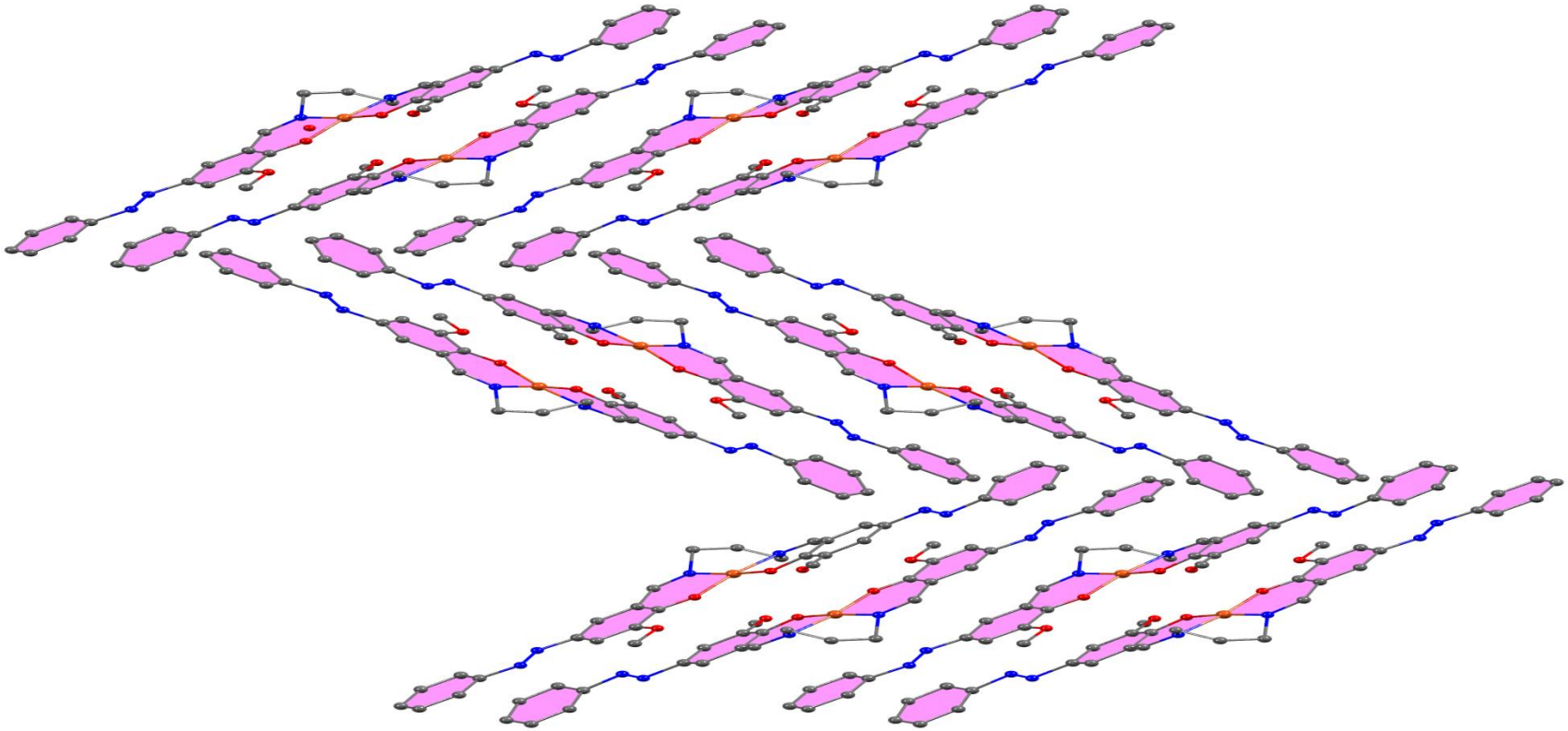

Fig.S3. Supramolecular architecture of complex **3** propagating along the *b axis* showing π–π stacking interaction and H-bondinginteraction. Hydrogen atoms of least interest are omitted for clarity.

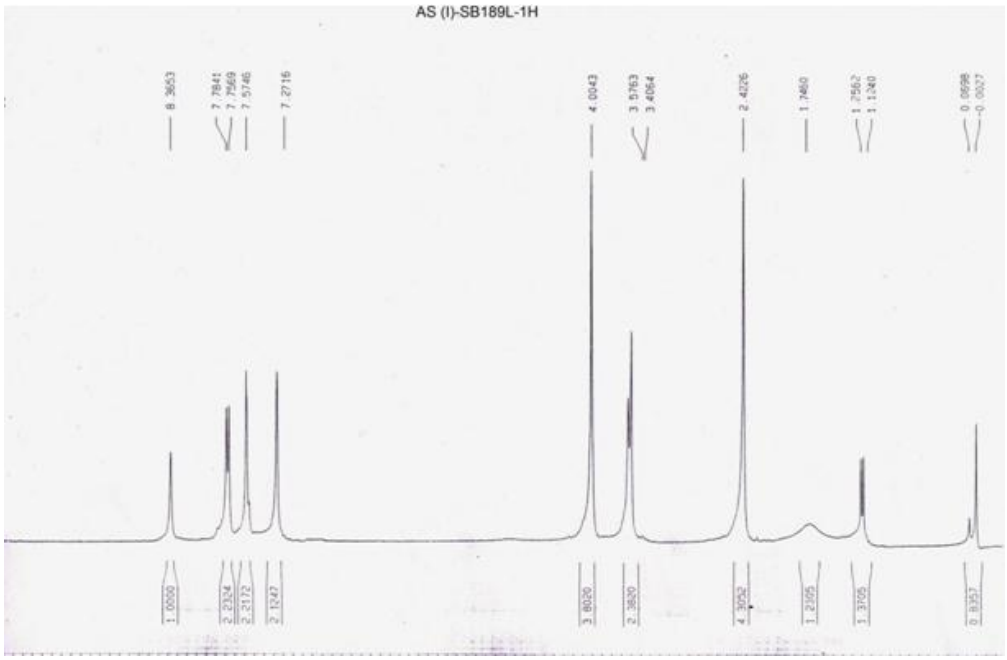

Fig. S4. ^{1}HNMR($CDCl_3$, 300 MHz) spectrum of $\mathbf{H_2L^1}$.

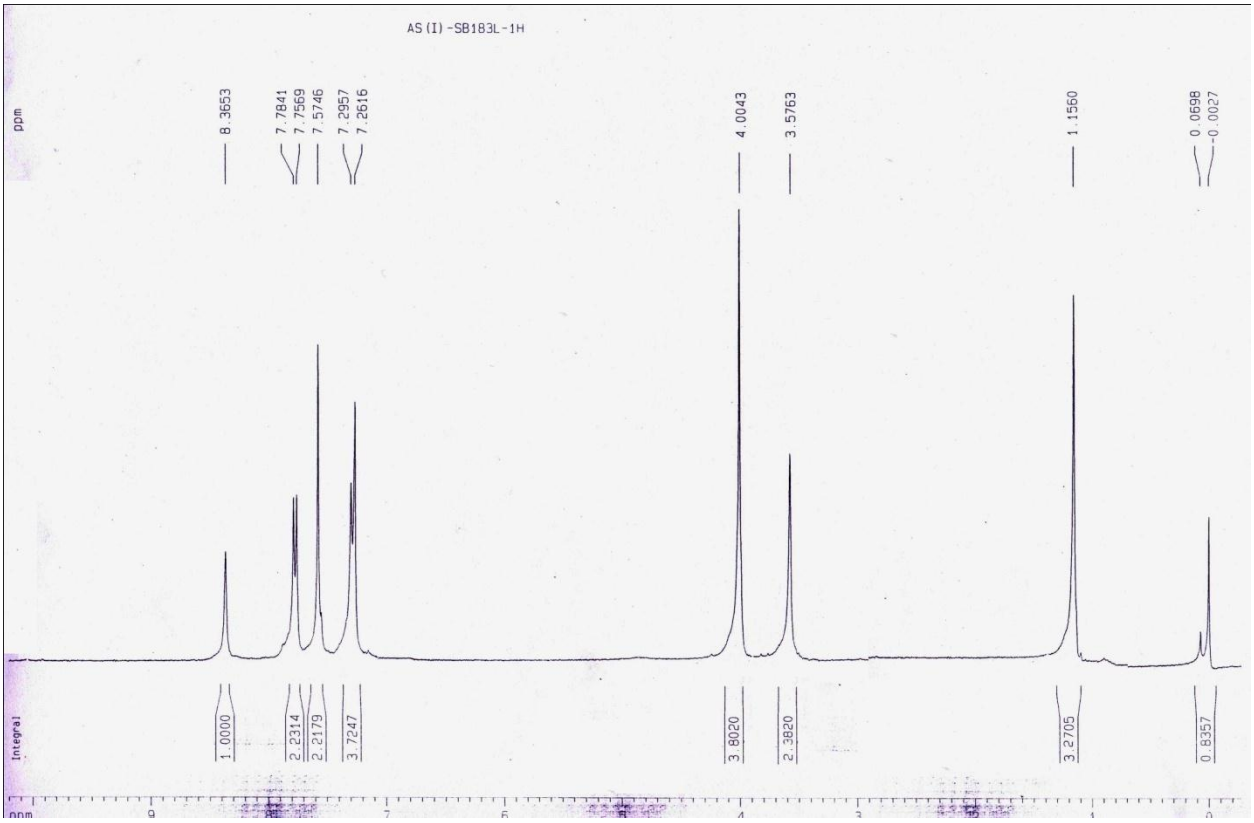

Fig. S5. ^{1}HNMR(d$_6$-DMSO, 300 MHz) spectrum of $\mathbf{H_2L^2}$.

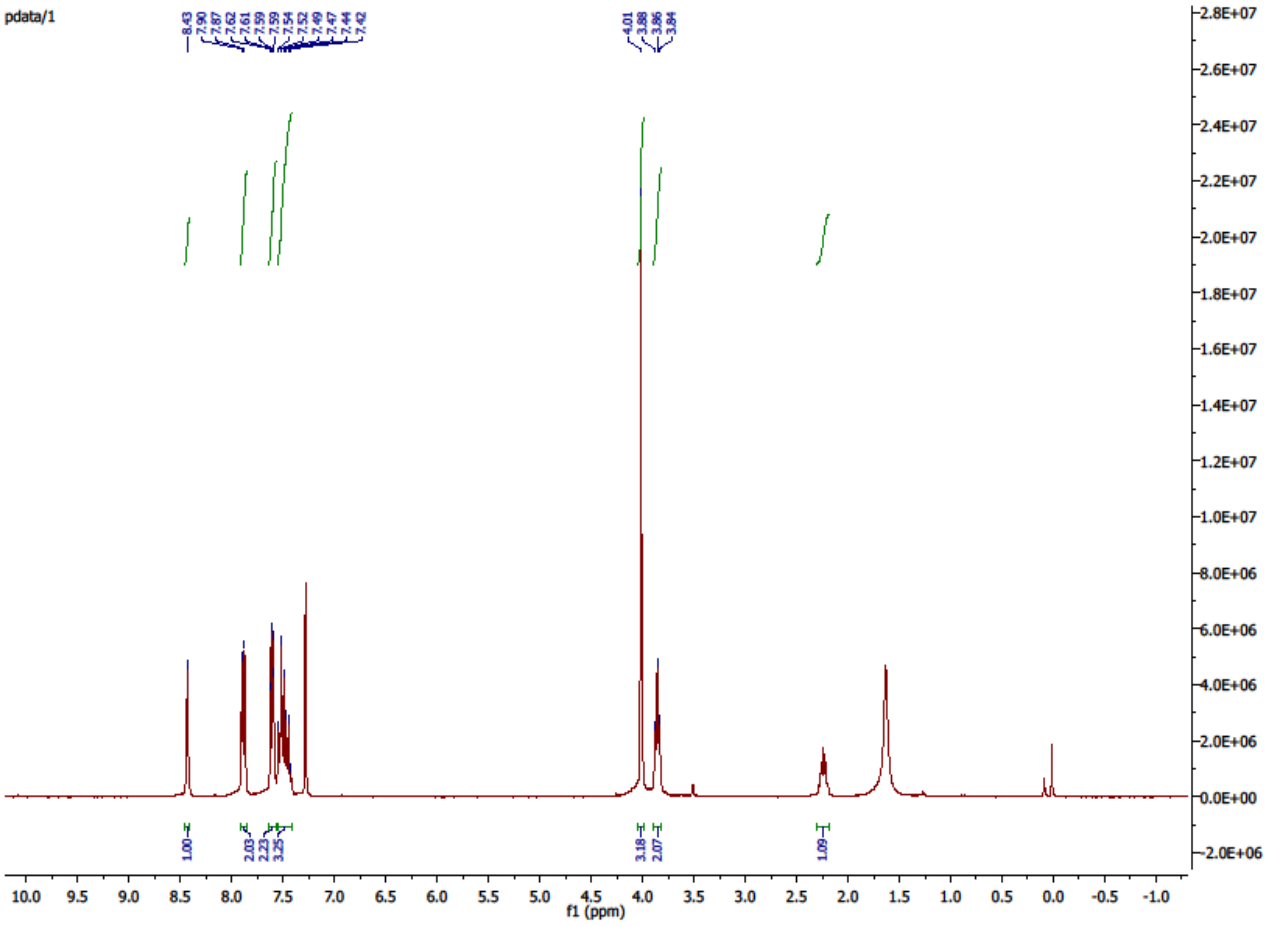

Fig. S6. ^{1}HNMR ($CDCl_3$, 300 MHz) spectrum of $\mathbf{H_2L^3}$.

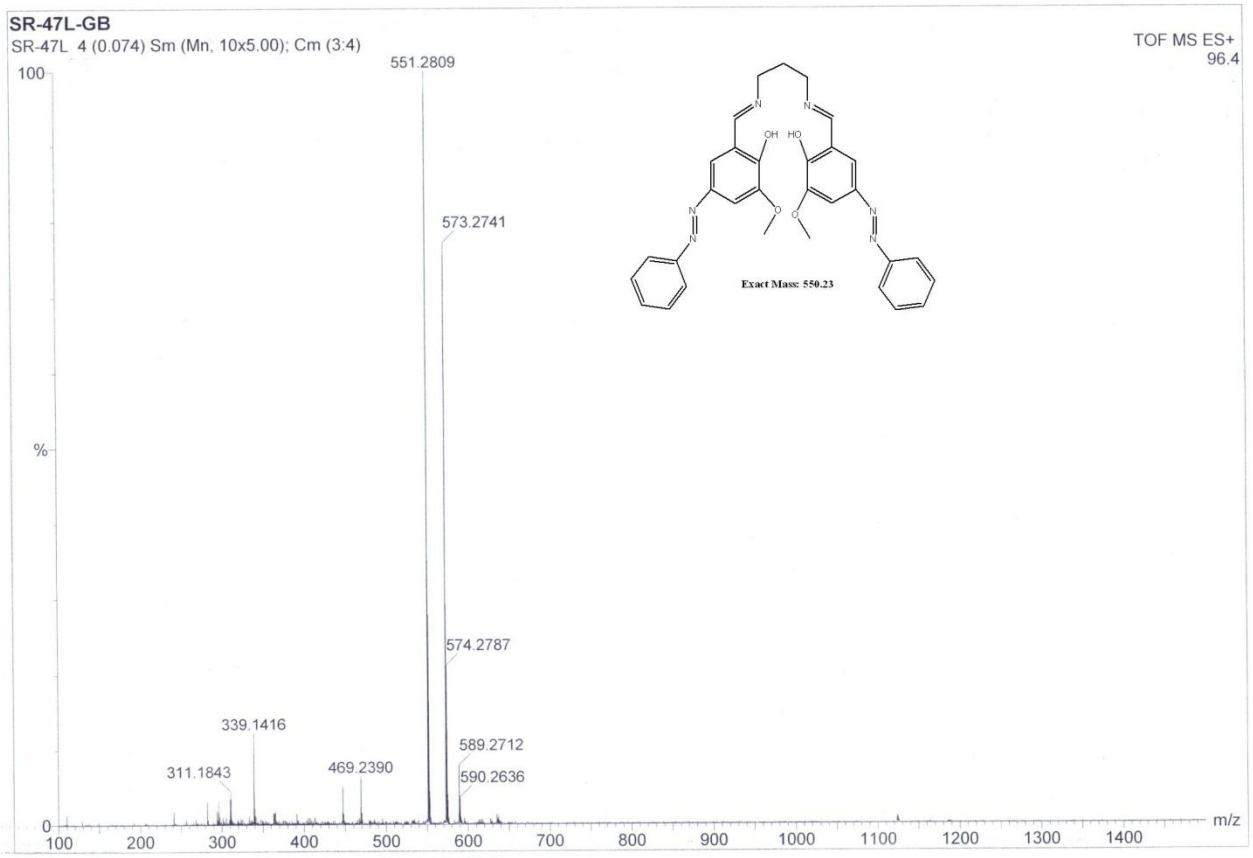

Fig. S7. Mass Spectrum of $\mathbf{H_2L^3}$.

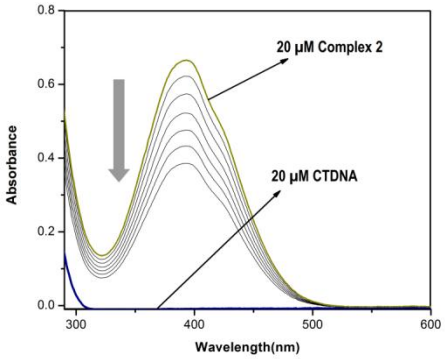

Fig. S8. UV-vis spectra of 2×10^{-5} (M) DNA with incremental addition of complex **2** (0-120 μM).

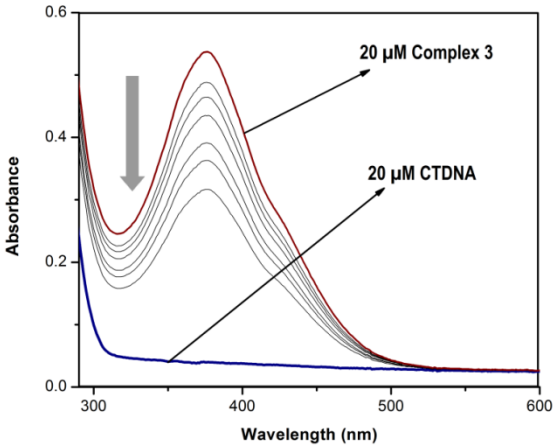

Fig. S9. UV-vis spectra of 2×10^{-5} (M) DNA with incremental addition of complex **3** (0-120 μM).

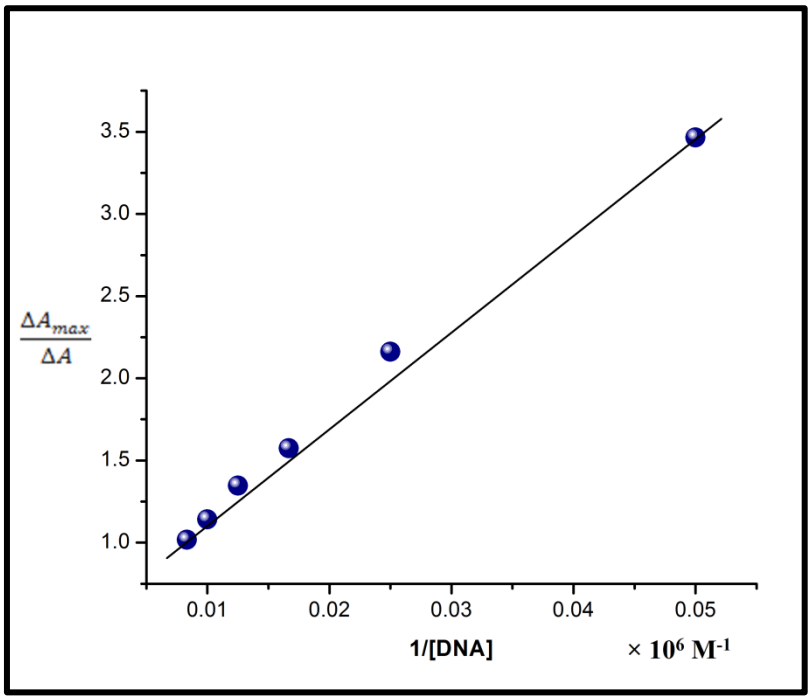

Fig. S10. Benesi Hildebrand equation for complex **1.**

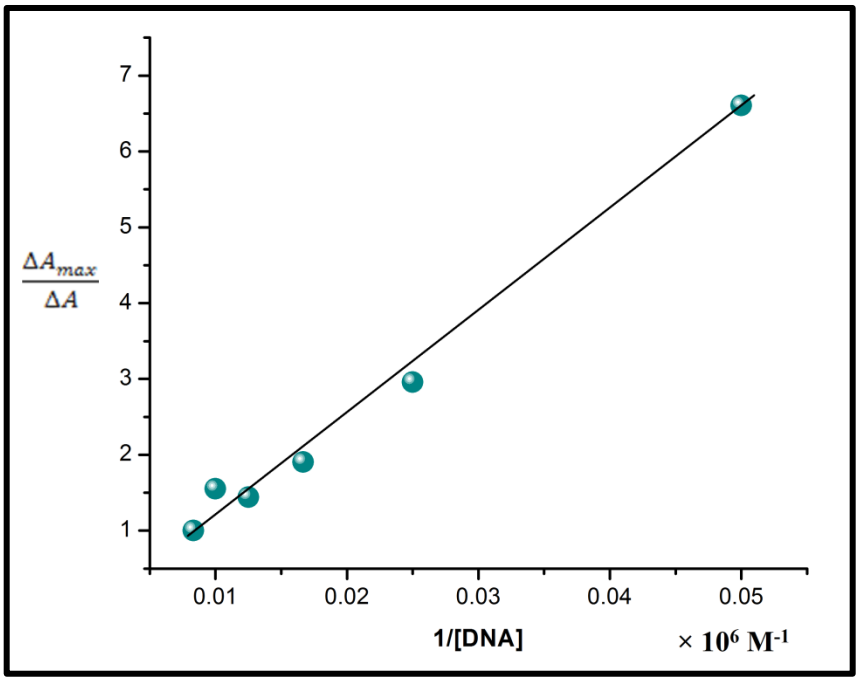

Fig. S11. Benesi Hildebrand equation for complex **2.**

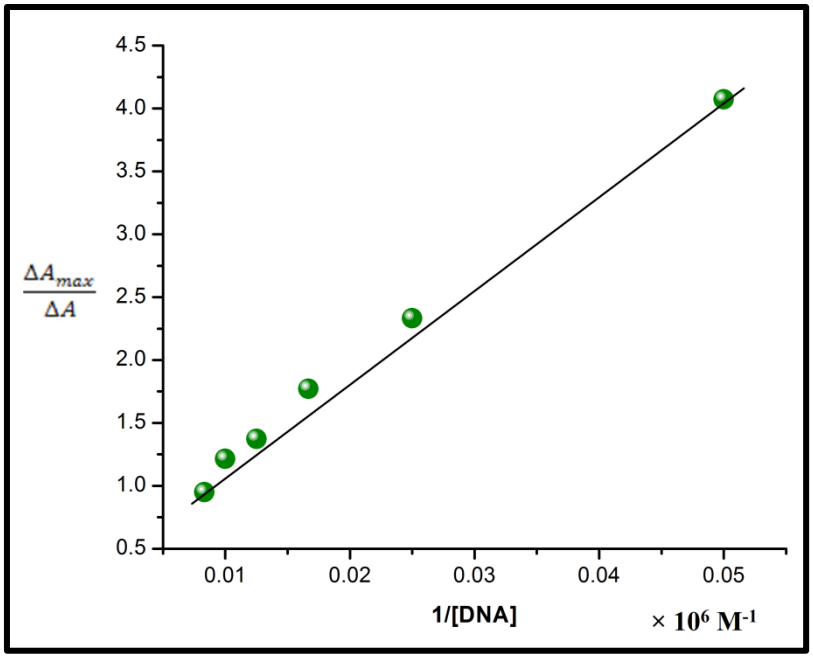

Fig. S12. Benesi Hildebrand equation for complex **3.**

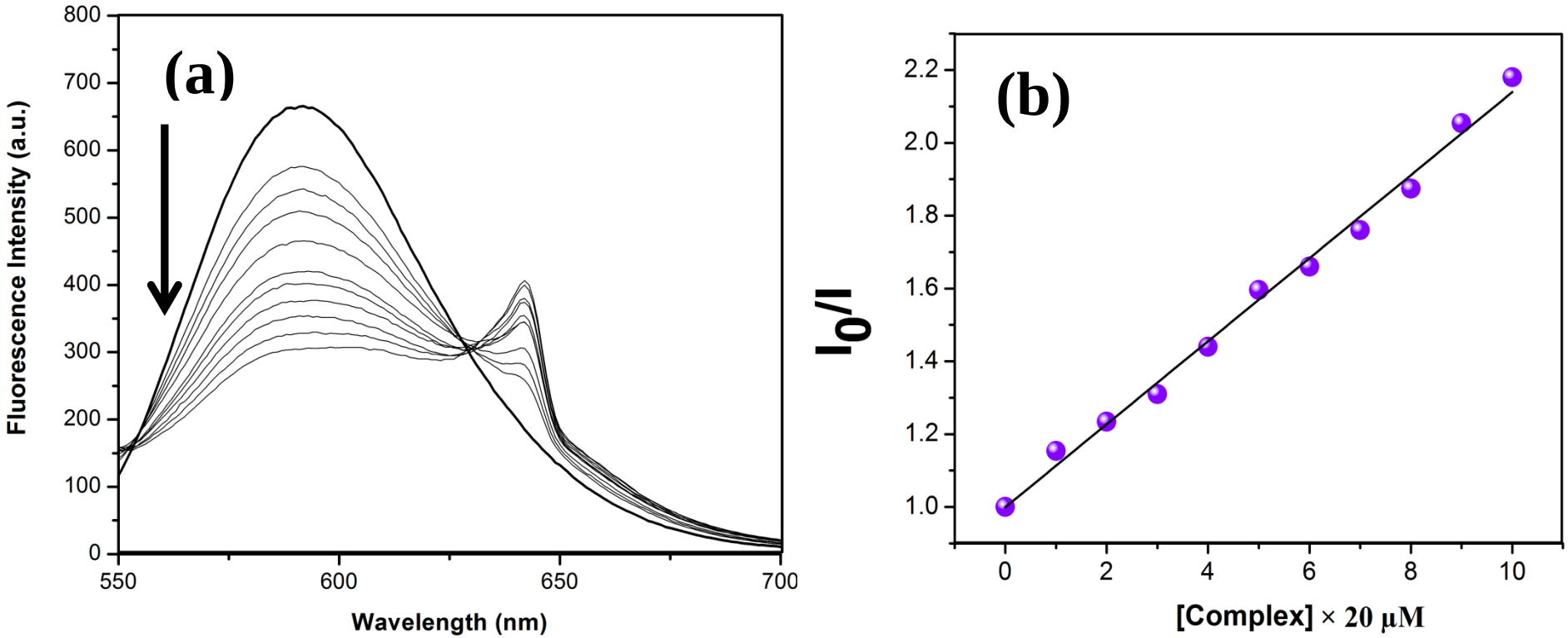

Fig. S13. Fluorescence spectra of (a) 20 μM EB bound DNA with incremental addition of complex **2** (0-120 μM). (b) Stern-Volmer plot for the quenching of fluorescence ofEthidium bromide (EB)-DNA complex caused by complex **2**.

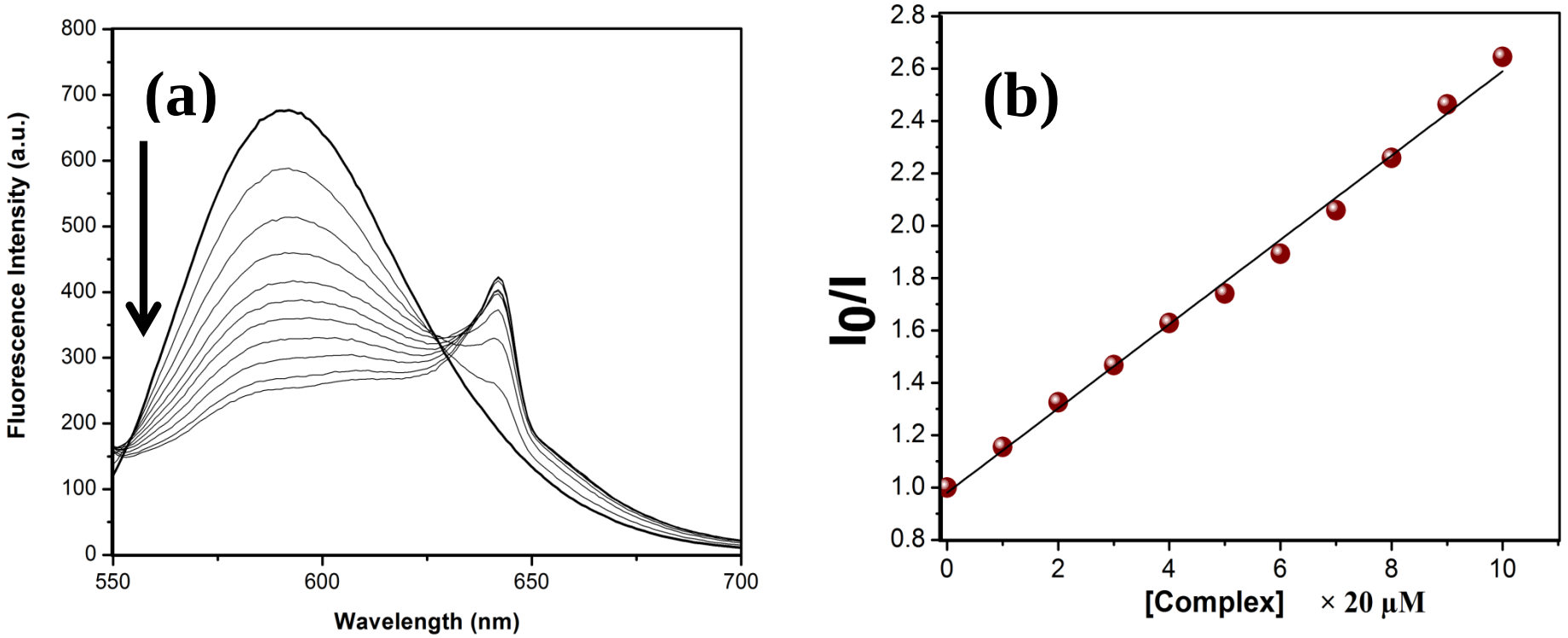

Fig.S14. Fluorescence spectra of (a) 20 µM EB bound DNA with incremental addition of complex **3** (0-120 µM). (b) Stern-Volmer plot for the quenching of fluorescence of Ethidium bromide (EB)-DNA complex caused by complex **3**.

Viscometric study

Viscometric measurements were carried out using a Cannon-Manning semi micro dilution viscometer type 75 (Cannon Instruments Co., State College, PA, USA) submerged vertically in a constant temperature bath maintained at 20±0.5 °C. Flow times of CT DNA solution in presence of increasing concentration of complexes **1**, **2** and **3** were measured in triplicate with an accuracy of ±0.01 s and the relative specific viscosity was calculated by using the equation:

$$\frac{\eta_{sp}^{'}}{\eta_{sp}} = \frac{[t_{complex} - t_0]}{[t_{control} - t_0]} \text{.....(1)}$$

Where, η'_{sp} and η_{sp} are the specific viscosity CT DNA in presence and in absence of complexes; $t_{complex}$ and $t_{control}$ are the time of flow of complex and control solution and t_o is the same for buffer solution.[1]

Viscosity Measurement

To evaluate the binding mode of interaction of complexes **1-3** with CT DNA, viscosity measurement was performed. This hydrodynamic method is just an apt way to assess the binding mode of small molecules to nucleic acids. Fig. 1 represents the effect of complexes **1-3** on the viscosity of CT DNA solution. During intercalation mode of binding, small molecules inserted in between bases of nucleic acids which causes elongation of helix chain length and this in turn increases the viscosity of solution.[2] On the other hand, Groove binding or electrostatic binding has no substantial effect on the viscosity of CT DNA solution.[3] In our case, we found that on binding with the three complexes, relative specific viscosity value of CT DNA solution did not alter and remains almost constant with increase in D/P ([Complex]/[CT DNA]) ratio. This observation clearly rules out the mode of binding to be intercalation and specifies the binding mode to be groove binding.

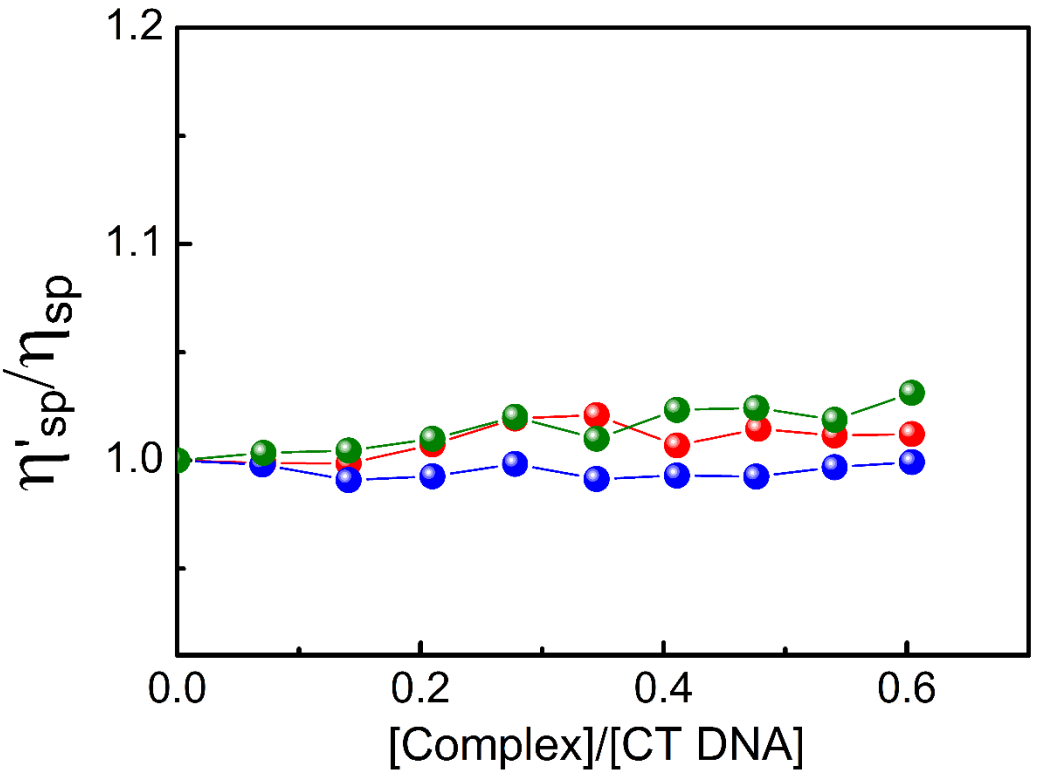

Fig. S15. Plot of change of relative specific viscosity of CT DNA in the presence complexes **1** (red circle), **2** (blue circle) and **3** (green circle) in 10 mM CP buffer of pH 7.0 at 25 °C. The concentration of CT DNA was 300 µM.

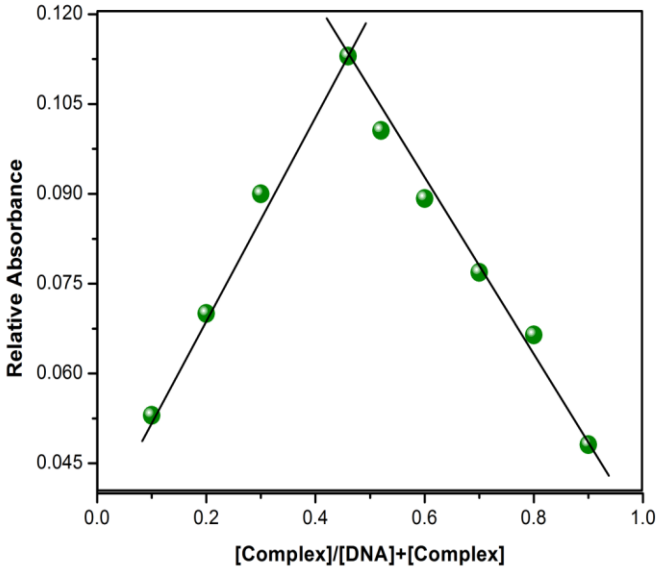

Fig. S16. Job's plot of complex **1**.

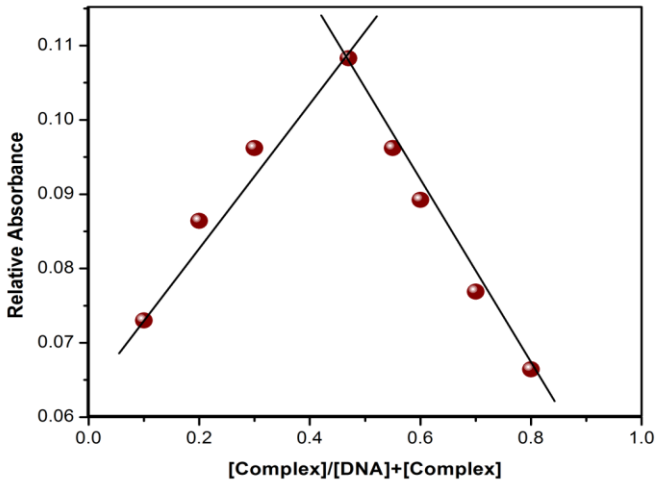

Fig. S17. Job's plot of complex **2**.

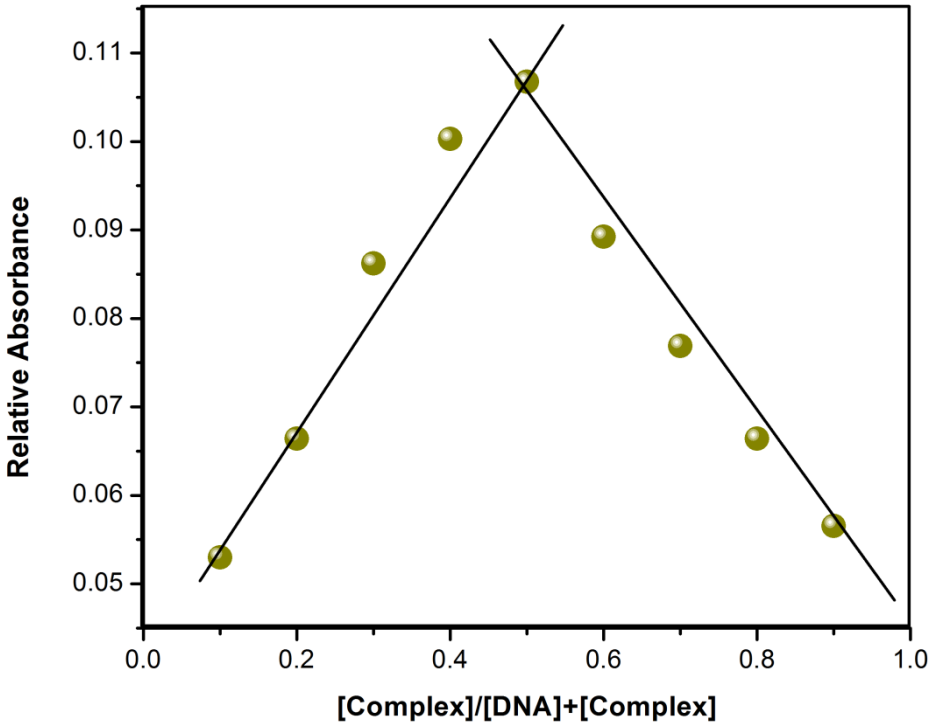

Fig. S18. Job's plot of complex **3**.

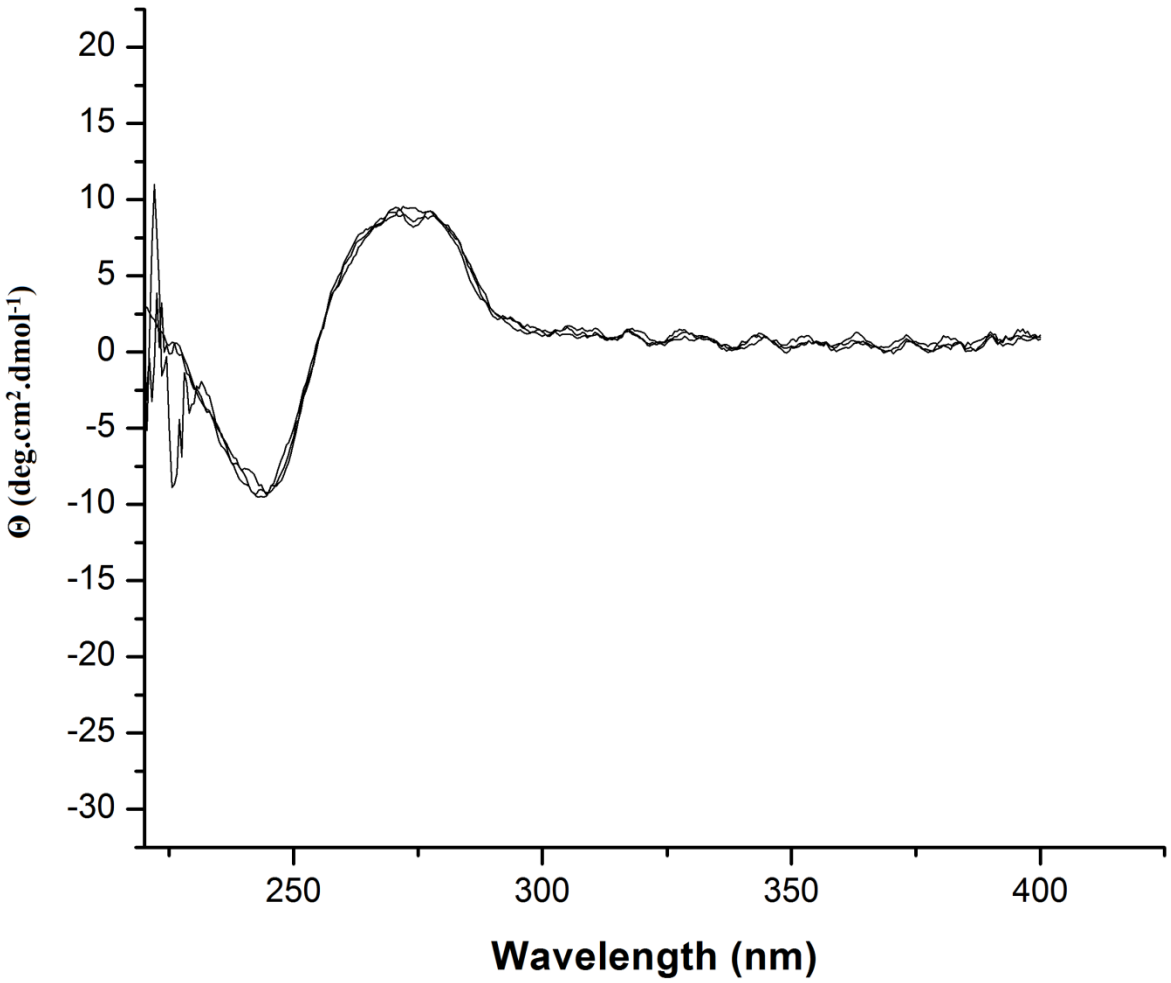

Fig. S19. CD spectra of CT DNA in absence and in presence of complex **1-3**.

M.O.s	(α-spin)	(β-spin)
LUMO+3	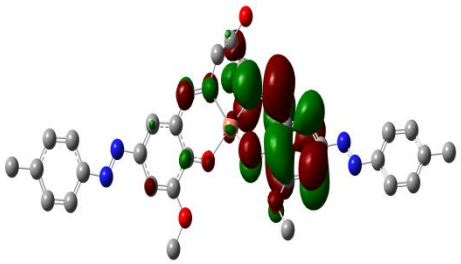	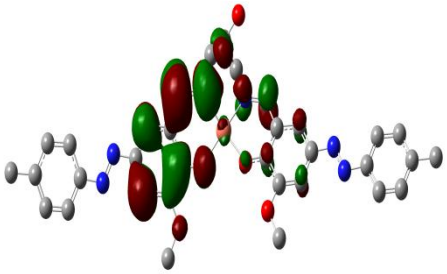
LUMO+2	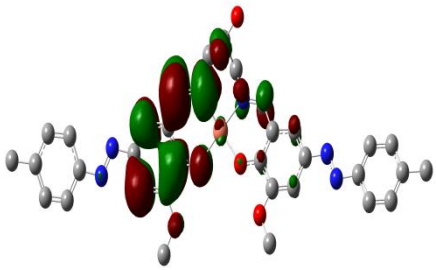	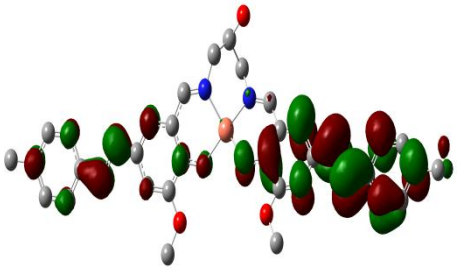
LUMO+1	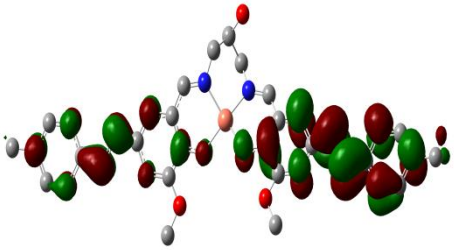	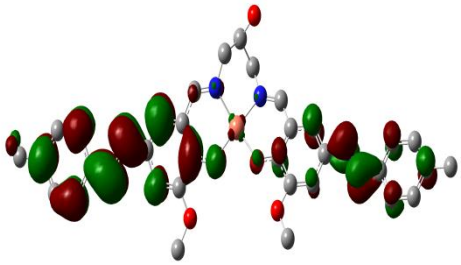
LUMO	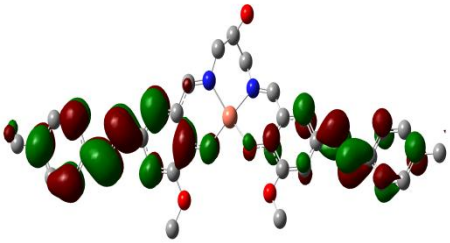	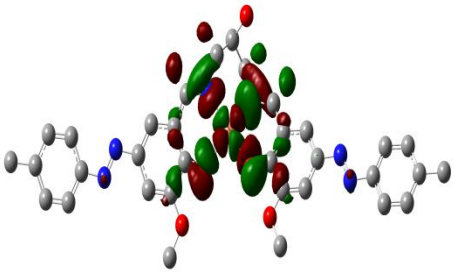

HOMO	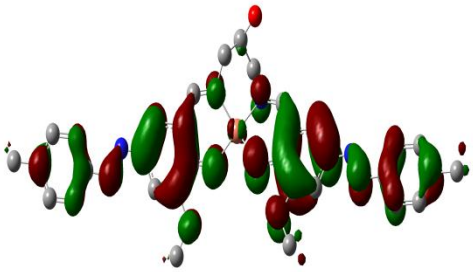	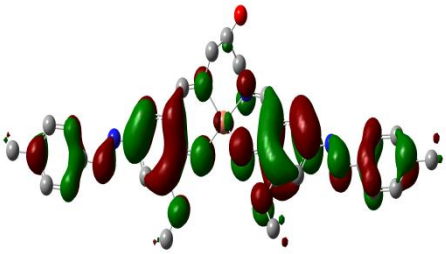
HOMO-1	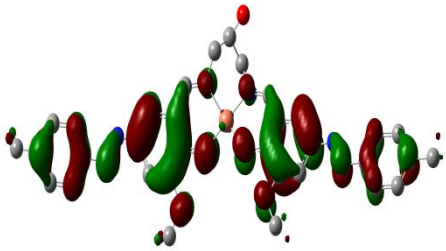	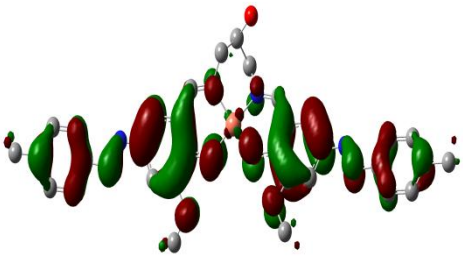
HOMO-2	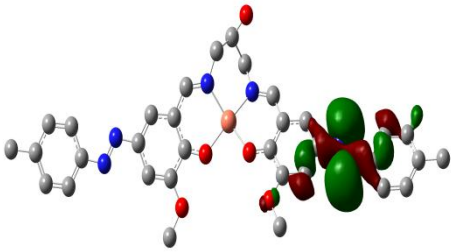	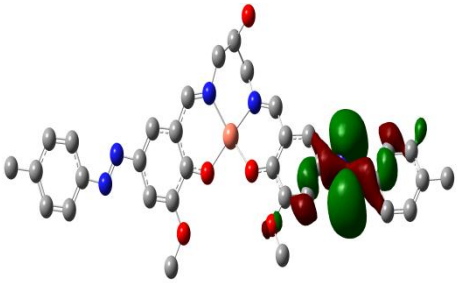
HOMO-3	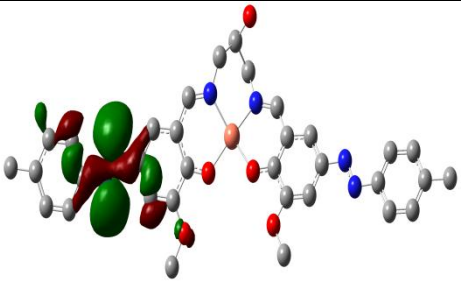	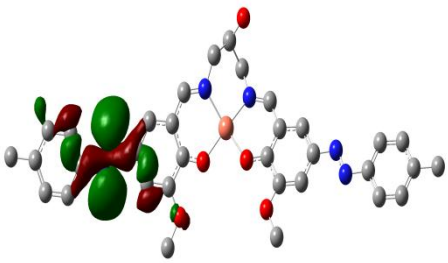

Fig.S20. Selected contour plots of molecular orbitals of complex **1.**

M.O.s	(α-spin)	(β-spin)
LUMO+3	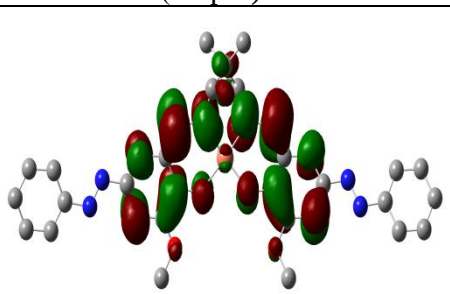	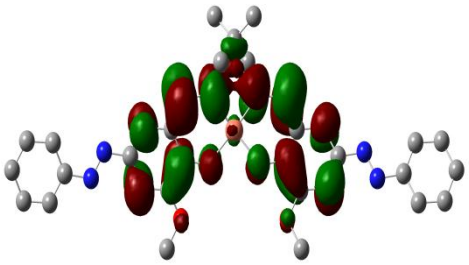
LUMO+2	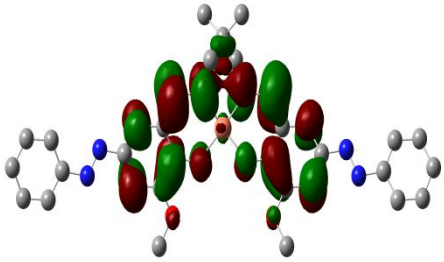	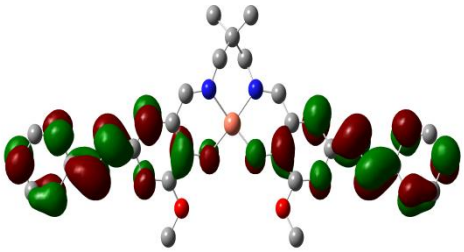
LUMO+1	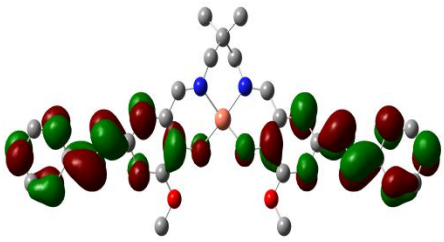	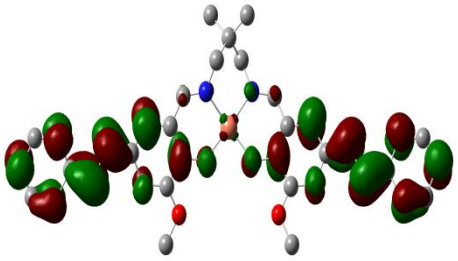
LUMO	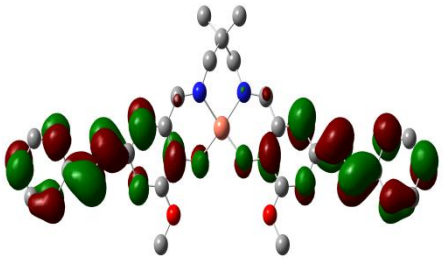	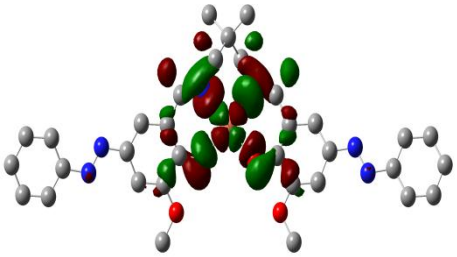

HOMO	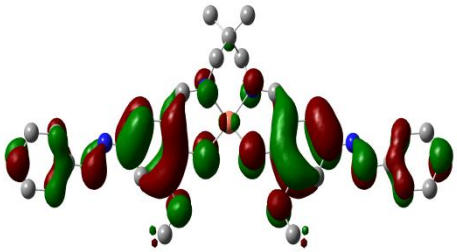	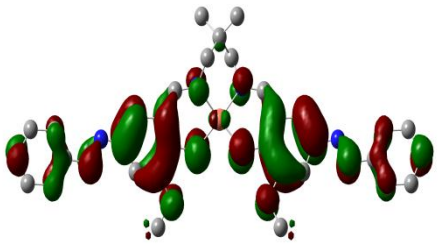
HOMO-1	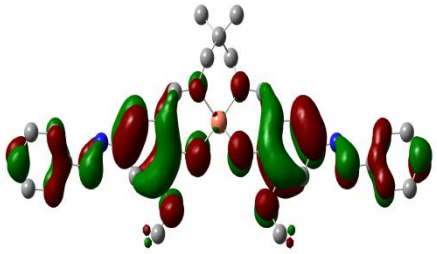	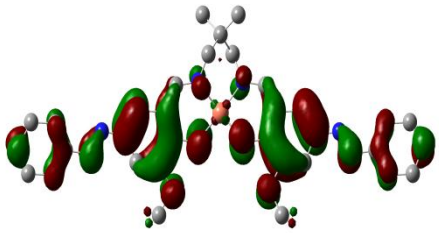
HOMO-2	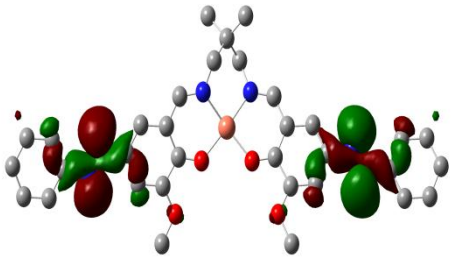	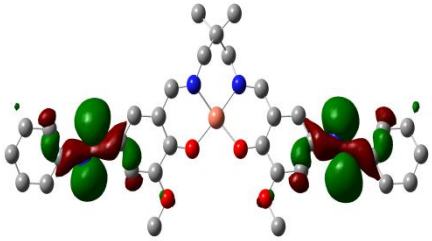
HOMO-3	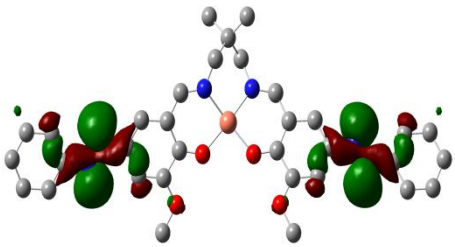	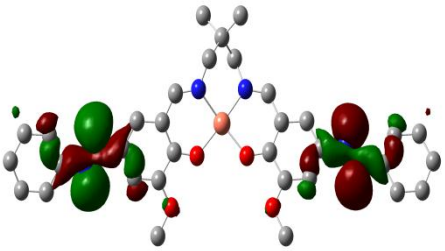

Fig. S21. Selected contour plots of molecular orbitals of complex **2.**

M.O.s	(α-spin)	(β-spin)
LUMO+3	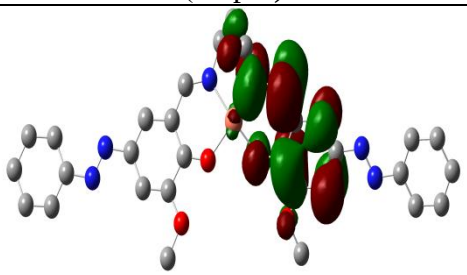	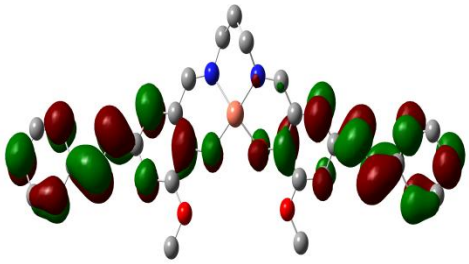
LUMO+2	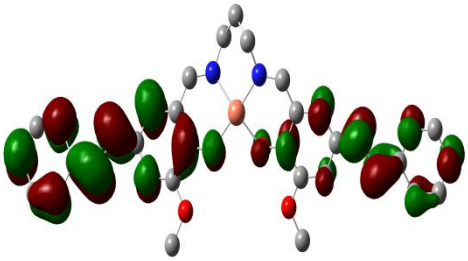	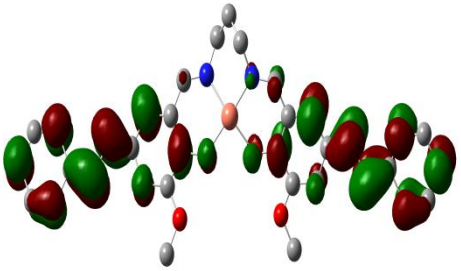
LUMO+1	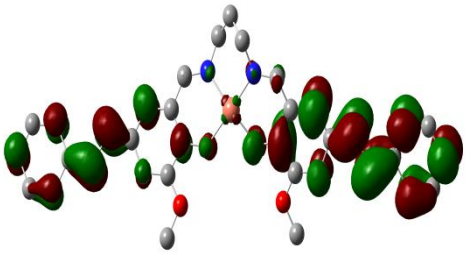	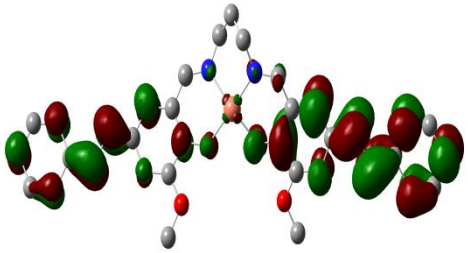
LUMO	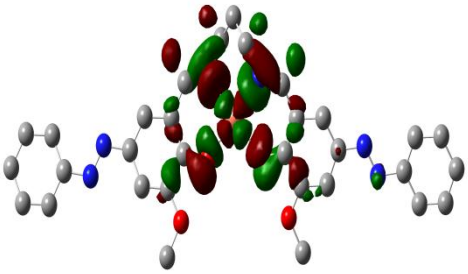	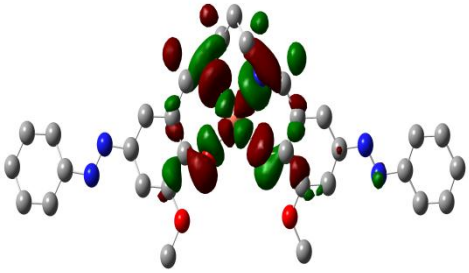

HOMO	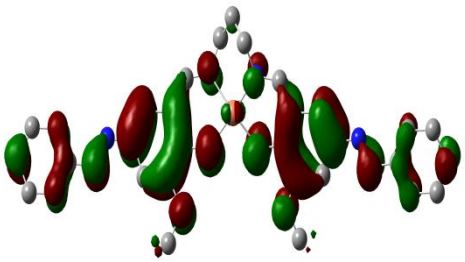	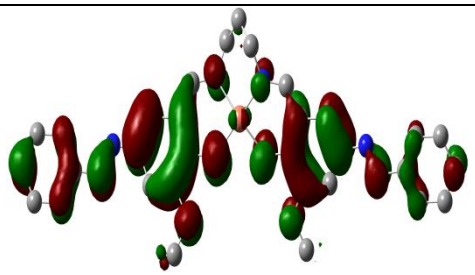
HOMO-1	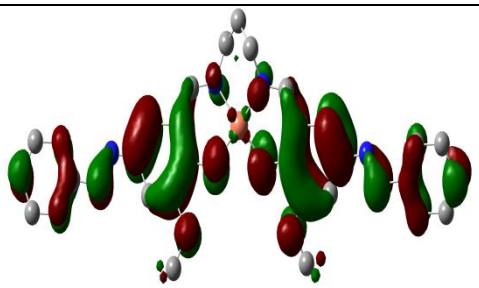	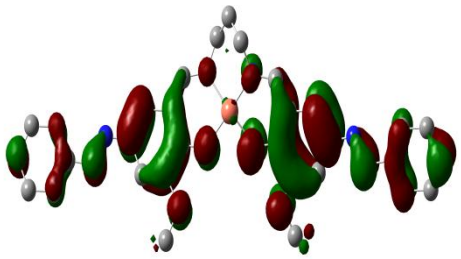
HOMO-2	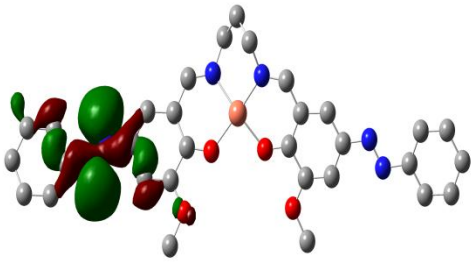	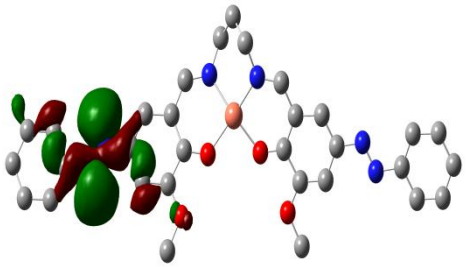
HOMO-3	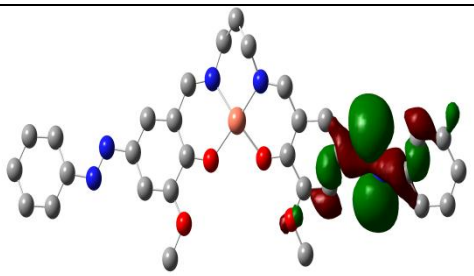	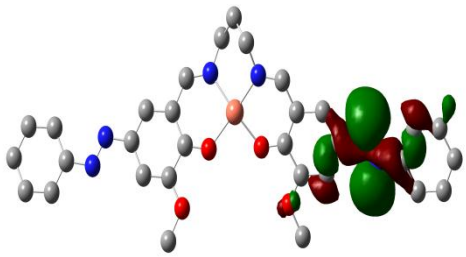

Fig.S22. Selected contour plots of molecular orbitals of complex **3.**

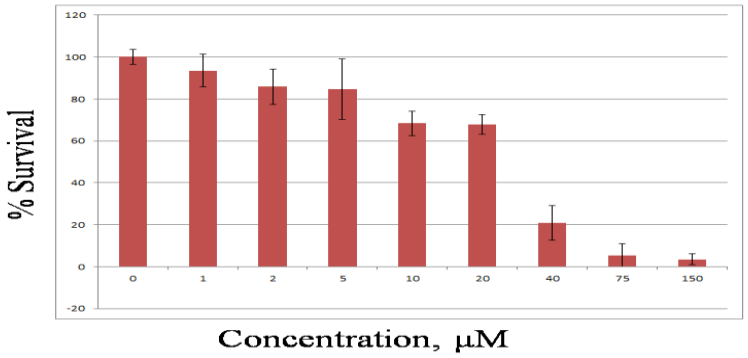

Fig. S23. Represents % cell viability of A549 cells treated with different concentrations (0–150 µM) of Complex **2** for 12 h determined by MTT assay. Results are expressed as mean of three independent experiments.

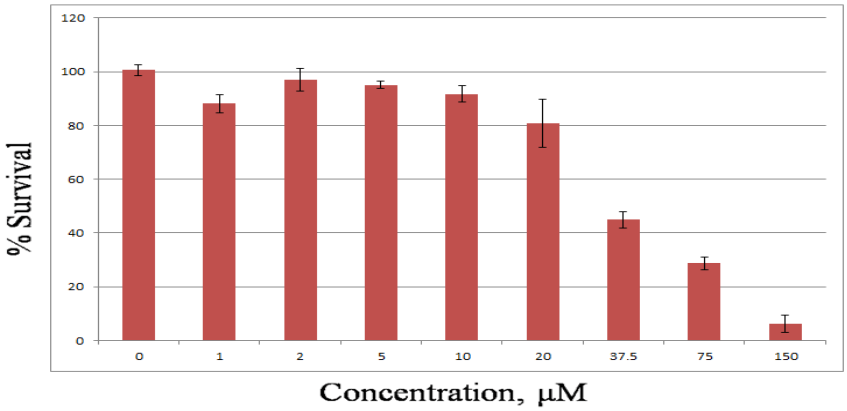

Fig. S24. Represents % cell viability of A549 cells treated with different concentrations (0–150 µM) of Complex **3** for 12 h determined by MTT assay. Results are expressed as mean of three independent experiments.

References

1 L. Haque, S. Bhuiya, R. Tiwari, A. B. Pradhan and S. Das, *RSC Adv.*, 2016, **6**, 83551–83562.

2 A. B. Pradhan, L. Haque, S. Roy and S. Das, *PLoS One*, 2014, **9**, 1–10, e87992.

3 A. B. Pradhan, L. Haque, S. Bhuiya, A. Ganguly and S. Das, *J. Phys. Chem. B*, 2015, **119**, 6916–6929.